ACS OMEGA

Open Access

http://pubs.acs.org/journal/acsodf

Article

Inhibition of JAK/STAT3 Expression by Acute Myeloid Leukemia-Targeted Nanoliposome for Chemotherapy Enhancement

Yao Zuo,[§] Hongwen Li,[§] Xiaochao Wang,[§] Yejin Liang, Caihong Huang, Guanye Nai, Jingrong Ruan, Wenzheng Dong, and Xiang Lu*

Cite This: *ACS Omega* 2024, 9, 37901−37909

Read Online

ACCESS | Metrics & More | Article Recommendations | Supporting Information

ABSTRACT: Acute myeloid leukemia (AML) is a relatively common malignant hematological disease whose development is mostly associated with abnormal activation of the JAK/STAT3 signaling pathway. Our previous study revealed that SAR317461, a novel JAK2/STAT3 inhibitor, can effectively inhibit the activation of the JAK2/STAT3 signaling pathway and has significant damaging and pro-apoptotic effects on AML cell lines. This project aims to build upon our prior research to enhance the application of SAR317461 in AML. The surface modification of liposomes with the CD34 antibody, along with the inclusion of the SAR317461 and cytarabine (a common AML chemotherapeutic agent), is observed. Due to the high expression of CD34 on the surface of AML cells, the nanoliposome could target AML cells specifically, further achieving an effective treatment for AML through the synergistic effect of JAK2/STAT3 inhibitors and chemotherapeutic agents. The implementation of this project will provide more theoretical support and ideas for the clinical application of JAK/STAT3 inhibitors in malignant tumors and for overcoming chemotherapy resistance.

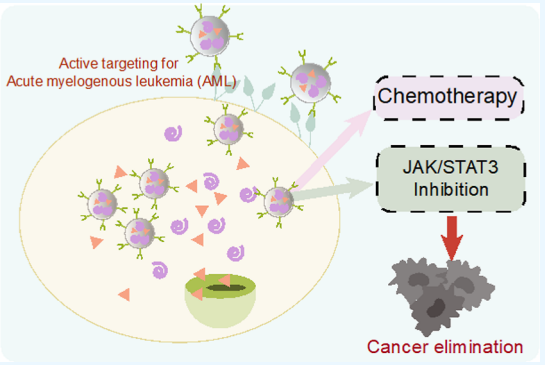

INTRODUCTION

Acute myeloid leukemia (AML) is a malignant hematologic cancer of myeloid hematopoietic stem/progenitor cells, primarily caused by the replacement of normal myeloid cells by leukemic cells.[1] As one of the more common malignant hematologic diseases in China, the main treatment for AML is traditional chemotherapeutic agents.[2] However, with issues such as multidrug resistance, molecular heterogeneity, and recurrence, it is urgent to present an effective therapeutic strategy for significant clinical effect development with high-tumor targeting efficacy. With the advancements in molecular biology, the inter- and intracellular signaling processes have gained attention in recent years.[3] As an important intracellular transcription factor, signal transducers and activators of transcription 3 (STAT3) are activated in vivo by phosphorylation of the upstream nonreceptor tyrosine kinase JAK kinase (Janus kinase), which is closely related to cell differentiation, proliferation, and apoptosis, and aberrantly activated STAT3 promotes tumor development.[4,5] Aberrant activation of STAT3 has been observed in multiple types of leukemia cells, and more prominent progress in clinical trials has been discovered in targeting JAK/STAT3 pathway inhibitors for leukemia therapy.[6,7] It has been shown that using JAK/STAT3-related pathway inhibitors to block the aberrant activation of this pathway or apply its chemotherapeutic drugs to tumor cells simultaneously can effectively improve the sensitivity of tumor cells to chemotherapeutic drugs and reduce multidrug resistance.[8−12] Therefore, the combination of this pathway inhibitor with conventional chemotherapeutic drugs is expected to play a more effective synergistic role in the treatment of drug-resistant, recalcitrant, and relapsed AML.

Among some common drug delivery systems, liposomes are favored for their biofilm-like structure, intravital degradability, and low immunogenicity.[13,14] The targeted high-density functional groups modification on liposomes surface and their inherent characteristics for drug release have led to an increasing application of liposomes in drug delivery.[14,15] CD34 is a receptor highly expressed on the surface of myeloid leukemia cells, whereas it is typically expressed on normal multifunctional hematopoietic stem cells.[16] Therefore, the application of CD34 antibody-mediated drug-loaded liposomes was used to target AML cells in this study.[17] Subsequently, the specific release of drugs from liposomes was achieved through synergy between JAK/STAT3 and chemotherapeutic drugs. This approach is anticipated to enhance the therapeutic effect of AML and have potential for clinical application.[18]

Received: May 5, 2024
Revised: August 10, 2024
Accepted: August 20, 2024
Published: August 28, 2024

Despite the significant progress in the analysis of various genetic mutations and phenotypes in AML over the past 40 years, there have been no obvious breakthroughs in the clinical management of AML compared to other hematologic tumors.[16] It has been found that abnormal activation of the JAK/STAT3 signaling pathway in tumors can promote drug resistance in tumor therapy.[13] Therefore, combining JAK/STAT3 inhibitors with other targeted therapies or conventional chemotherapeutic agents is expected to reduce drug resistance and achieve synergistic therapeutic effects. Thus, in this study, the most commonly used cytarabine (chemotherapeutic drug for AML) and SAR317461 (a novel inhibitor) were designed to synergistically treat AML (Figure 1).

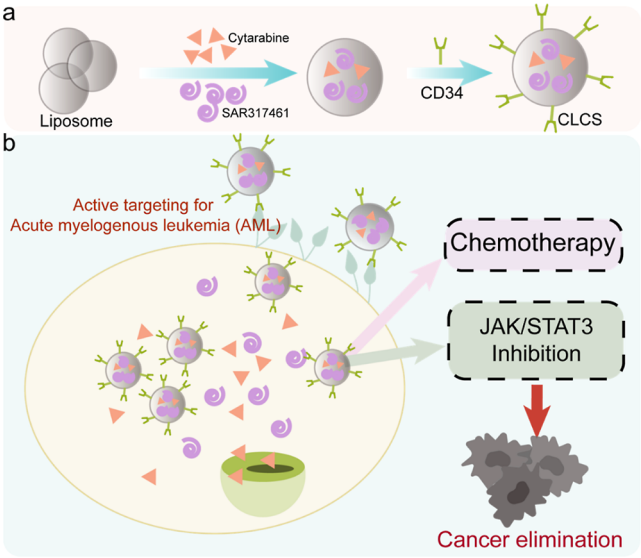

Figure 1. Schematic diagram of nanoliposome for chemotherapy synergy JAK/STAT3 inhibition against AML. (a) Schematic illustration of the synthesis process of CLCS nanoliposome. (b) Schematic diagram of CLCS-mediated chemotherapy and JAK/STAT3 pathway inhibition for AML therapy. After active targeting of CLCS for AML, the released cytarabine resulted in AML cells death, and the inhibited JAK/STAT3 by SAR317461 further caused cancer elimination.

Furthermore, liposomes grafted with CD34 antibodies were used as a drug delivery system for more effective AML cell targeting, which equipped with high CD34 receptor expression and were able to inhibit the overproliferation of AML cells specifically. The implementation of this study will provide more clinical ideas for the treatment of AML and more malignant tumors and will further provide more theoretical support to solve the problem of chemotherapy resistance, for promoting the clinical application of JAK/STAT3 signaling pathway inhibitors and the development of molecular medicine.

RESULTS AND DISCUSSION

Synthesis and Characterization of CLCS Nanoliposome. As reported, liposomes with cytarabine and SAR317461 loading and with CD34 antibody coating (denoted as CLCS), liposomes with cytarabine and SAR317461 loading and without CD34 antibody coating (denoted as LCS), and liposomes with SAR317461 loading and with CD34 antibody coating (denoted as CLS) were obtained. As observed in Figure 2a, transmission electron microscopy (TEM) images clearly revealed the spherical morphology of CLCS, with 100 nm diameter of particles. Therewith, dynamic light scattering (DLS) was used to determine the hydrodynamic sizes and zeta potentials of CLS, LCS, and CLCS (Figure 2b,c). Compared to CLS (about 106 nm), the results from the hydrodynamic sizes of CLCS (about 142 nm) demonstrated that cytarabine was successfully loaded into the liposome. In the process of drug loading and CD34 antibody modification, the stepwise alteration of zeta potentials also verified the successful loading of drugs and coating of CD34 antibody. Next, the loading rates of cytarabine and SAR317461 were measured by high-performance liquid chromatography (HPLC). CLCS revealed remarkable drug encapsulation capacity with loading rates of 54.7% (cytarabine) and 49.2% (SAR317461), respectively. Furthermore, the stability of CLCS nanoliposome was evaluated by hydrodynamic size analysis through DLS in PBS and 10% serum solution during 14 days (Figure 2d,e). With drug loading and CD34 antibody coating, CLCS nanoliposome could keep an excellent dispersibility without sediment over time. As shown in Figure 2f, the drug release rate of hydrolysis of CLCS liposomes was accelerated at pH 5.4, while cytarabine and SAR317461 were both released sustainably. After 48 h incubation, the cumulative release rate of cytarabine reached approximately 86%, and the cumulative release rate of SAR317461 reached about 58%. Subsequently, flow cytometry was applied for CD34 modification analysis outside the nanoliposomes. The most amount of CD34 was observed in CLCS groups, which indicated the available decoration in CLCS (Figure 2g,h). Then, confocal laser scanning microscopy was carried out for CD34 antibody modification. As shown in Figure 2i, the majority of red fluorescence representing CD34 were emerged on CLS and CLCS, showing that the associated antibodies on the surface of membrane were reserved on CLS and CLCS. The presence of this antibody in CLS and CLCS rather than LCS further confirmed the CD34 modification, endowing the nanoliposome with AML nidus targeting properties.

CLCS Nanoliposome Generated Cytotoxicity and JAK/STAT3 Inhibition In Vitro. Previous studies have depicted that the tumor cell membrane associated antibody camouflaged nanoparticles could be recognized by homologous tumor cells, increasing tumor targeting delivery efficiency specifically.[14] Thus, cellular uptake effects of CLCS in AML cells were observed by confocal fluorescence microscopy. After coincubation with Cy5-labeled LCS or CLCS, C1498 cells were investigated, which showed stronger red fluorescence in CLCS-treated cells, indicating the enhanced cellular uptake effects of CLCS than that of LCS (Figure 3a). Also, the flow cytometer analysis results were consistent with the consequences above (Figure 3b,c). These results indicated the specific targeting viability of CLCS to the CD34 overexpression tumor cells.

Furthermore, the antitumor ability of CLCS was monitored by live/dead cell staining. Red fluorescence signals were obviously observed in live/dead cell staining pictures, proving that CLCS could cause tumor cell death availably (Figure 3d). More importantly, apoptosis/necrosis staining assays revealed the powerful AML cell killing ability of the CLCS (Figure 3e,f).

Then, Western blot analysis was carried out for the expression of pJAK2, JAK2, pSTAT3, and STAT3 in AML cells after various treatments. As depicted in Figure 3g, the majority of bands of above proteins was observed in the PBS group, to the contrary the expression of the above proteins

https://doi.org/10.1021/acsomega.4c00710
ACS Omega 2024, 9, 37901−37909

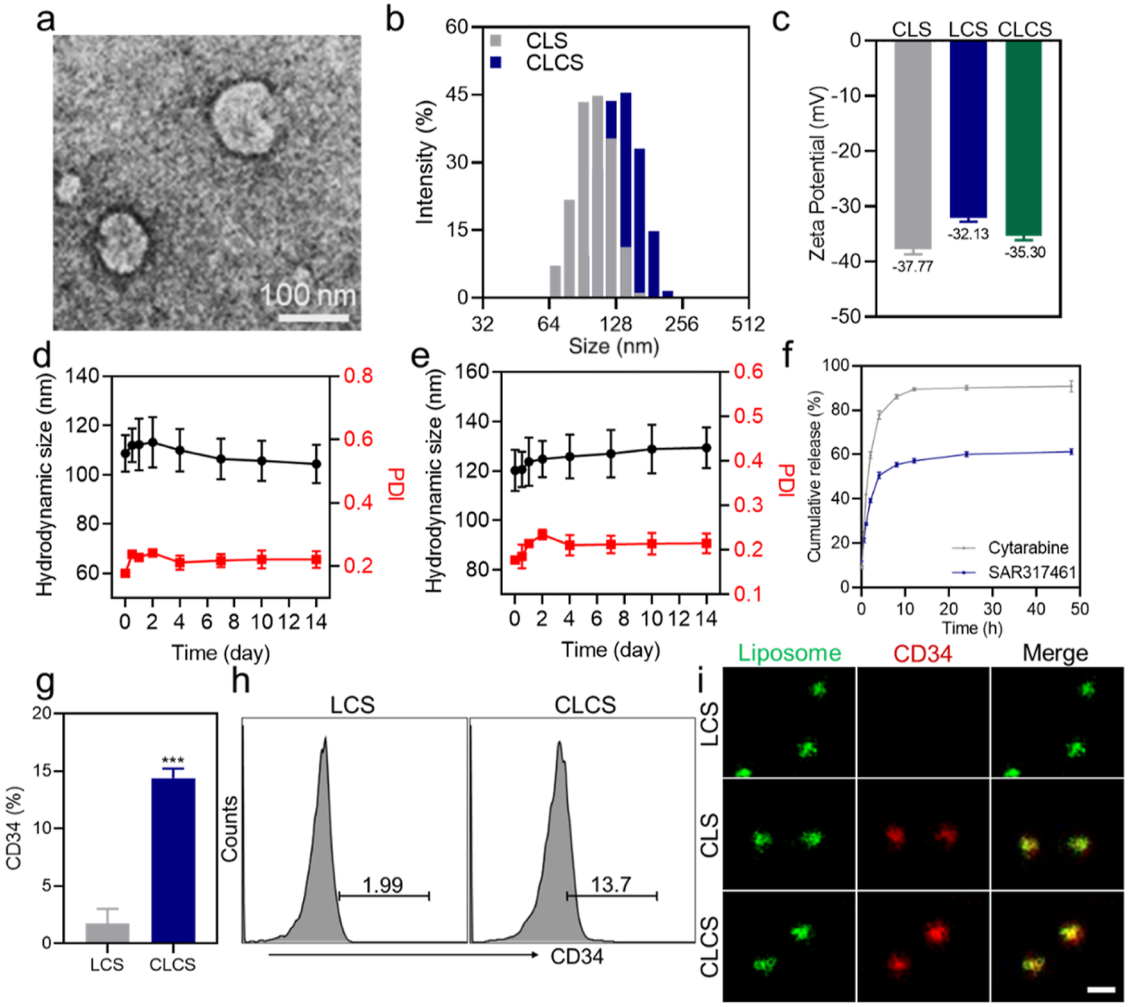

Figure 2. Characterization of CLCS nanoliposome. (a) TEM image of CLCS. (b) Hydrodynamic sizes of CLS and CLCS. (c) Zeta potentials of CLS, LCS, and CLCS. (d,e) Size and PDI of CLCS in PBS and serum solution for 14 days for stability assessment. (f) Drugs release rate from CLSC during 48 h (n = 3). (g) Quantification of CD34 in AML cells after LCS or CLCS coincubation by flow cytometry. (h) Ratio of CD34 after LCS or CLCS coculture in AML cells. (i) Confocal fluorescence pictures of LCS, CLS, and CLCS nanoliposomes (green: liposome, red: CD34). Scale bar: 150 nm. *p < 0.05, **p < 0.01, and ***p < 0.001.

after CLCS incubation was appeared, demonstrating that CLCS could inhibit the JAK/STAT3 signaling pathway, which was in accordance with the consequence in Figures S1 and S2. Next, the cytotoxicity of nanoliposome toward AML cells was examined by MTT assay, which revealed that CLCS treatment displayed the strongest cell death ability in Figure 3h. These results suggested that such antibody decorated nanoliposome could promote the delivery efficiency of drugs to accumulate in tumor cells and improve the antitumor effect significantly.

In Vivo Targeted and Therapeutic Effect of CLCS. The targeting capability of CLCS in vivo was evaluated in AML-bearing mice. As depicted in Figure 4a, the signal of CLCS could be obviously observed in the femur distinctly than that of LCS. The ex vivo quantitative fluorescence intensity of main organs and femur also testified the stronger aggregated ability of CLCS at the tumor region than LCS (Figure 4b,c). The results of the pharmacokinetics assay displayed that CLCS equipped a favorable blood circulation ability compared to that of LCS (Figure 4d). The amounts of white blood cells (WBCs) in leukemic mice were enhanced suddenly than that of healthy mice. After treatments, blood samples from mice were collected for hematological analysis, and the counts of WBC in the CLCS group were decreased visibly compared to the PBS group, indicating the alleviation of symptoms in AML-bearing mice after CLCS administration (Figure 4e). Subsequently, the percentages of $CD34^+$ cells were decreased in the CLCS group, which proofed the eradication of AML cells by CLCS (Figure 4f,g). As shown in Figure 4h, the spleens were collected after treatment, spleen weights were measured, and the group of CLCS revealed obviously reduced splenomegaly. Besides, the therapeutic effect of CLCS in leukemic mice was investigated by the photographs of the femur. The whole femur was distinctly pale in the PBS group, revealing the serious damage of the femur under leukemia. Oppositely, the femurs after CLCS treatment were shown original dark red (Figure 4i), which further proved the antitumor effect of CLCS. Meanwhile, the body weights curves and survival situation of AML-bearing mice were recorded during the treatment. The body weights of PBS, CLS, and cytarabine-treated groups were decreased rapidly, which might be contributed by the weak leukemia and toxicity of chemotherapeutic drugs. Also, the body weights of other groups were decreased, indicating the biosecurity of these nanoliposome to some extent (Figure 4j). Besides, the overall

https://doi.org/10.1021/acsomega.4c00710
ACS Omega 2024, 9, 37901−37909

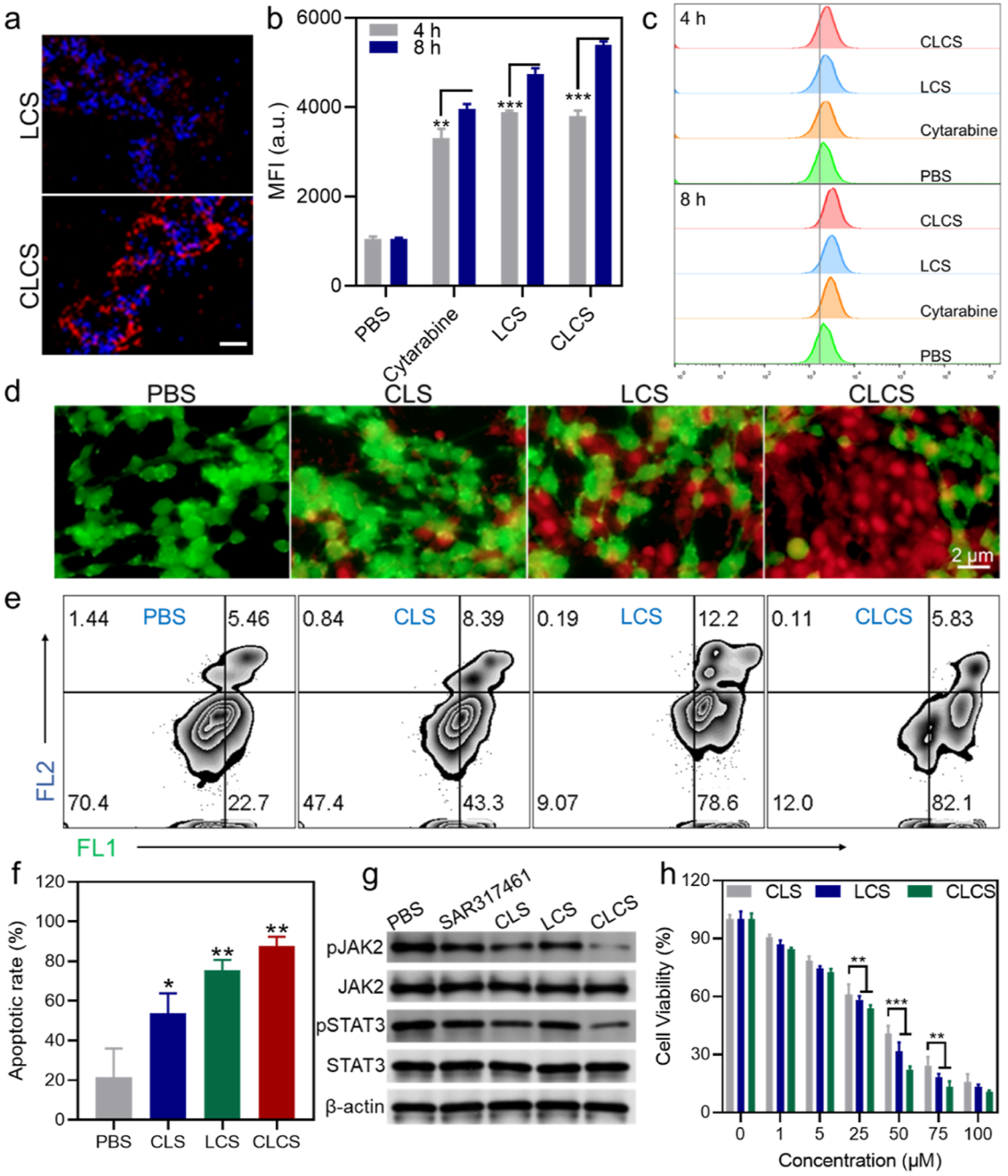

Figure 3. In vitro cytotoxicity of CLCS nanoliposome. (a) Confocal fluorescence pictures of cell uptake of nanoliposomes (blue: cell nucleus, and red: LCS or CLCS). Scale bar: 500 nm. (b) Quantification of cell uptake of nanoliposomes through flow cytometry at different time points. (c) Representative flow cytometric images of C1498 cell uptake of nanoliposomes after being treated with LCS and CLCS for 4 and 8 h. (d) Dead/live staining of C1498 cells after various treatments (green: live cells, and red: dead cells). (e) Apoptosis/necrosis analysis of C1498 cells after multifarious treatments by flow cytometry. (f) Quantification of apoptotic cell after various treatments. (g) Western blotting analysis of JAK2/STAT3 expression in AML cells after sorts of treatments. (h) Cell viability of C1498 cells after multiple treatments. *$p < 0.05$, **$p < 0.01$, and ***$p < 0.001$.

survival rate depicted by CLCS could prolong the survival time more than 60 days. The overall survival of PBS was 22 days; meanwhile, the survival rates of SAR317461, cytarabine, and CLS were declined rapidly among 30 days. However, the mice after CLCS treatment were survived more than 60 days, revealing the satisfactory effect of CLCS to prolong the survival time of AML-bearing mice (Figure 4k).

Biosafety Assay of CLCS. For investigating the biosecurity of CLCS, H&E staining of main organs, blood biochemistry analysis, and blood routine test were performed. The H&E staining of major organs after various treatments demonstrated the low systemic toxicity of CLCS (Figure S3). The liver function-associated markers were maintained in normal ranges (Figure 5a,b). Also, as shown in Figure 5b,c, negligible changes were noticed in kidney function-related markers. Furthermore, the main blood cells were recorded after multiple treatments by blood routine tests (Figure 5g–i). The densities of main blood cells were sustained at steady extents. These hematological tests revealed that there was no remarkable host toxicity of CLCS in vivo.

https://doi.org/10.1021/acsomega.4c00710
ACS Omega 2024, 9, 37901−37909

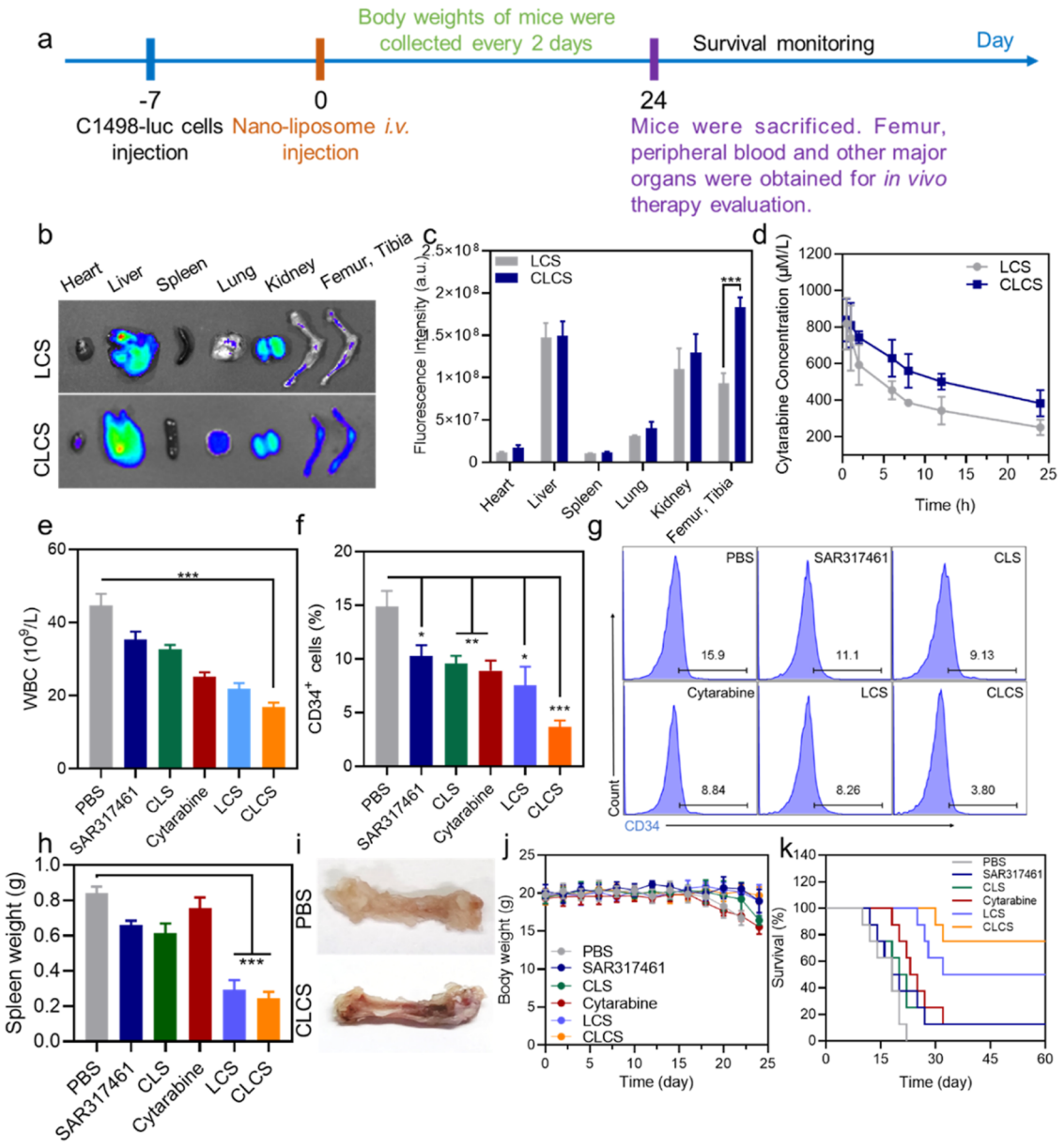

Figure 4. In vivo targeting and antitumor effect assay of CLCS nanoliposome. (a) Construction of AML bearing murine model and treatment plans in vivo. (b) Ex vivo fluorescence pictures and quantification (c) of AML-bearing mice after LCS and CLCS administration at 8 h (n = 3). (d) Pharmacokinetics curves of cytarabine after intravenous administration with LCS or CLCS nanoliposome (n = 3). (e) Amounts of WBC in peripheral blood in AML-bearing mice after multiple treatments (n = 3). (f) Quantity and representative flow cytometry plots (g) of the $CD34^+$ cells in AML-bearing mice after multiple treatments (n = 3). (h) Weights of spleens from AML-bearing mice after receiving sorts of treatments (n = 3). (i) Images of mice femurs from AML-bearing mice to identify the leukemic cells in vivo. (j) Body weight curves in AML-bearing mice administrated by various nanoliposomes during 24 days (n = 8). (k) Survival curves of AML-bearing mice after nanoliposomes injection (n = 8). *p < 0.05, **p < 0.01, and ***p < 0.001.

CONCLUSIONS

Based on the domestic and international research on the JAK/STAT3 signaling pathway and its inhibitors, this study proposes to utilize the novel inhibitor SAR317461 as a potentiating drug for chemotherapy enhancement to improve the sensitivity of AML cells to chemotherapeutic drugs and increase the proportion of apoptosis of tumor cells. Combined with chemotherapeutic drugs, the precise targeting of AML cells through CD34 antibody-mediated drug-loaded liposomes can decrease the drug resistance of cells and further reduce the dose of chemotherapeutic drugs and their side effects on normal cells to a certain extent. This study innovatively combines the novel JAK2/STAT3 inhibitor SAR317461 with the commonly used AML chemotherapy drug cytarabine for the treatment of AML, which improves the therapeutic effect of the inhibitor on AML to a certain extent while reducing chemotherapy resistance and side effects.

MATERIALS AND METHODS

Materials and Cell Lines. Cytarabine, tricaprin, and DSPE-PEG2000-Amine were purchased from Aladdin Reagent Co. Ltd. Mouse anti-CD34 monoclonal antibody (Clone: QBEND/10), penicillin−streptomycin, fetal bovine serum (FBS), Roswell Park Memorial Institute (RPMI) 1640

https://doi.org/10.1021/acsomega.4c00710
ACS Omega 2024, 9, 37901−37909

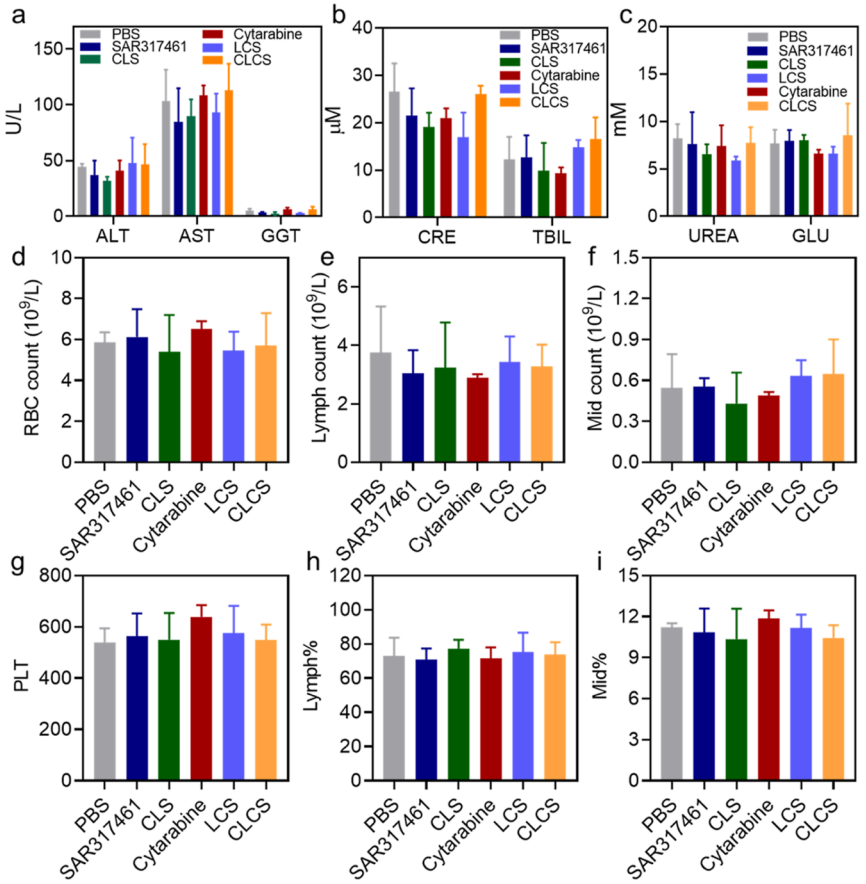

Figure 5. Biosafety of nanoliposomes by blood biochemistry and routine analysis in healthy mice. (a–c) Blood biochemistry tests in peripheral blood in healthy mice for control and treated groups (n = 3). (d–i) Blood routine examinations in healthy mice after various treatments (n = 3).

medium, and trypsin were obtained from Invitrogen (USA). Anti-JAK2 antibody (O60674), anti-JAK2/3 (phospho-Tyr966/939) antibody (O60674/P52333), anti-STAT3 antibody (P40763), and anti-STAT3 (phospho-Y705) antibody (P40763) were purchased from Bosterbio (China). SAR317461, Hoechst 33342, and 3-(4,5-dimethylthiazol-2-yl)-2,5-diphenyltetrazolium bromide (MTT) were purchased from Beyotime Biotechnology (China). C1498, a type of AML cell line, was supplied from the American Type Culture Collection (ATCC). C1498 cell line and luciferase-tagged C1498 (C1498-luc) cells were incubated in RPMI 1640 with 10% FBS and penicillin–streptomycin (100 U/mL) in an incubator at 37 °C under 5% CO_2.

Animal Models. All animal studies were abided by the protocols by the Affiliated Hospital of Youjiang Medical University for Nationalities. All experimental processes were performed following the Youjiang Medical University for Nationalities (Animal Ethics: 2021103001). All animals were supplied by the Youjiang Medical University for Nationalities. All animals were anaesthetized by isoflurane and sacrificed by CO_2-euthanasia under animal ethics.

Synthesis of CLCS. The ammonium sulfate gradient loading method was used to encapsulate the inhibitors SAR317461 and cytarabine. Soy lecithin (S100), cholesterol (Chol), and distearoylphosphatidylethanolamine-polyethylene glycol 2000 (DSPE-PEG2000-Amine) were dissolved in chloroform in a 20:5:1 molar ratio, and the chloroform was removed by overnight vacuum to form lipid films. Liposomes were then prepared by adding ammonium sulfate solution and a hydration reaction for 30 min. The liposome solution was repeatedly squeezed with a film extruder (average pore size: 0.4, 0.2, and 0.1 μm) and dialyzed in 10 mM histidine/10% sucrose for at least 36 h to obtain blank liposomes. Then, PEG-modified CD34 antibody was prepared by first reacting DSPE-PEG2000-Amine with N,N'-succinimidyl carbonate (DSC) under stirring to obtain DSPE-PEG2000-DSC, which was mixed and reacted with CD34 antibody to obtain PEG-modified CD34 antibody. Then, the blank liposomes were mixed with CD34 antibody in the mass ratio of 200:1 and incubated for 24 h under stirring. In summary, empty liposomes were formulated from a blend of S100/Chol/DSPE-PEG2000-Amine/tricaprin (at a ratio of 20:5:1:2, w/w/w) for encapsulating SAR317461 and cytarabine, with the variation of utilizing 250 mM ammonium sulfate as the hydration medium. Extrinsic ammonium sulfate was eliminated through dialysis against 10 mM histidine/10% sucrose (for SAR317461) and 5 mM HEPES/5% dextrose (for cytarabine). The drug-loaded liposomes were purified by a Sephadex G-50 dextran gel column to obtain CD34-modified drug-targeted liposomes.

Characterization of Nanoliposomes. TEM (JEOL JEM 2100F) was used to observe the morphology of the CLCS. DLS (Zetasizer Nano) was used for the assessment of hydrodynamic sizes and zeta potentials of different nanoliposomes. Western blotting analysis was used to evaluate the inhibition of JAK2/STAT3 in AML cells. In detail, AML cells were collected and lysed, after which the total protein contents were evaluated for further analysis. Amounts of protein per

https://doi.org/10.1021/acsomega.4c00710
ACS Omega 2024, 9, 37901–37909

sample (e.g., 50 μg) were loaded onto an SDS-PAGE gel with appropriate sample loading buffer (such as Laemmli 2x sample buffer). 10% Tricine-SDS-PAGE and the Bio-Rad Mini Protean gel electrophoresis system were used for Western blotting analysis. Next, the Bio-Rad Semi-Dry Blotter was used for transferring to nitrocellulose membranes for 10 min before blotting. Primary antibodies were incubated with samples in TBS-T for 1 h. Then, samples were washed with TBS-T three times along with secondary antibody solution applied in TBS-T for 1 h at room temperature. Developing solution was added and agitated gently for 10 min. Next, the developing solution was poured off and rinsed in several channels of distilled water when bands reached the desired intensity.

The CLS, LCS, and CLCS were incubated with fluorescein isothiocyanate overnight at 25 °C, along with the Rhodamine B-labeled CD34 antibody was decorated on the CLS and CLCS. The fluorescent distributions of LCS, CLS, and CLCS were analyzed by confocal laser scanning microscopy to observe the existence of CD34 antibody outside the CLCS.

SAR317461 and Cytarabine Loading and Releasing. A solution of SAR317461 (at a drug/liposome ratio of 0.35) and cytarabine (at a drug/liposome ratio of 0.2) was dispersed into the liposomal solution and coincubated for 1 h under 55 °C. The encapsulated drugs in the liposomes were divided from the free drugs by dialysis (using a 10 kDa cutoff membrane) overnight at 4 °C. The concentrations of loaded drug were quantified by HPLC after liposomes disruption in a 100-fold volume of ethanol. The encapsulation efficiency (EE) was calculated as follows: $EE = (W_1 - W_2)/W_1 \times 100\%$.

Where W_1 represents the total weight of drugs, and W_2 is the weight of free drugs in the supernatant.

CLCS was dispersed in PBS (pH 5.4) buffers in the dialysis tube, and the dissolved medium was collected at different time points for releasing drugs measurement by HPLC.

In Vitro Cell Uptake Assays. C1498 cells were seeded into the confocal dish with a density of 1×10^6 cells/mL for 24 h. Then, fluorescently labeled LCS and CLCS were coincubated with C1498 cells for several times. After that, the supernatants of C1498 cells were removed, and cell nuclei were stained with Hoechst 33342 for 20 min. The fluorescence of nanoliposomes was analyzed by a confocal microscope.

Also, C1498 cells were seeded into the six-well plates at a density of 1×10^6 cells/mL for 24 h culturation. Then, cytarabine, LCS, and CLCS were added and coincubated for different time points. Afterward, cells were collected for the endocytosis analysis by flow cytometry.

In Vitro Cytotoxicity Assay. C1498 cells were seeded in 96-well plates with the density of 1×10^4 cells/mL and cultured for 24 h. Then, the cells were incubated with sorts of concentrations of CLS, LCS, and CLCS nanoliposomes for 24 h. After that, 20 μL of MTT solution (5 mg/mL) was added for 4 h incubation, then the supernatant was removed, and 150 μL of DMSO was added for formazan dissolution. The optical density of solution in 570 nm was detected by a microplate reader.

Cell Death Mechanism Assays. 1×10^6 cells/mL C1498 cells (1×10^6 cells/mL) were seeded into six-well plates for 24 h incubation. After that, PBS, CLS (with equivalent dosages of 30 μM SAR317461), LCS (with equivalent dosages of 30 μM cytarabine), and CLCS (with equivalent dosages of 30 μM cytarabine) were added and coincubated for another 12 h. Then, the supernatants of C1498 cells were removed and used for further tests. The cells were stained with 5 μL of calcein AM (4 μM) and 10 μL of PI (4 μM) for 20 min and then observed by a fluorescence inverted microscope for live/dead cell staining. Meanwhile, the pretreated cells were stained with PI and Annexin V-FITC for 15 min and analyzed by flow cytometry for cell apoptosis and necrosis assay.

C1498 cells were seeded into six-well plates at a density of 1×10^6 cells/mL for 24 h incubation. After 24 h incubation, the cells were treated with PBS, SAR317461 (30 μM), CLS (with equivalent dosages of 30 μM SAR317461), LCS (with equivalent dosages of 30 μM cytarabine), and CLCS (with equivalent dosages of 30 μM cytarabine) and coincubated for further 24 h. Subsequently, the treated-C1498 cells were collected and washed with PBS three times for Western blotting analysis to evaluate the expression of the JAK2/STAT3 pathway.

In Vivo Biodistribution Assay. The AML-bearing mice were randomly divided into two groups ($n = 3$). LCS or CLCS was coincubated with Cy5-NHS at 25 °C overnight for fluorescence labeling. After Cy5 labeling, the mixtures were washed with ultrapure water three times to remove free Cy5. Cy5-labeled LCS (5 mg/kg) and CLCS (5 mg/kg) were injected into the leukemic mice. The fluorescence signals of the main organs and femur in mice were monitored by IVIS after 8 h of administration.

Pharmacokinetics Assay. Leukemic mice were randomly divided into two groups ($n = 3$). After that, the AML-bearing mice were administrated with LCS (5 mg/kg, with equivalent dosages of 3 mg/kg cytarabine) and CLCS (5 mg/kg, with equivalent dosages of 3 mg/kg cytarabine) intravenously. Blood samples of each mouse were obtained through the tail vein at different time points (1, 2, 6, 8, 12, and 24 h). The concentrations of cytarabine were detected by HPLC.

In Vivo Antileukemia Treatment in the Mice Model. C57BL/6J mice were used to establish the leukemia model. 10^5 C1498-luc cells were injected into C57BL/6J mice intravenously. After 7 days, mice were divided into six groups randomly ($n = 8$) and treated with PBS, SAR317461 (3 mg/kg), CLS (5 mg/kg, with equivalent dosages of 3 mg/kg SAR317461), cytarabine (3 mg/kg), LCS (5 mg/kg, with equivalent dosages of 3 mg/kg cytarabine), and CLCS (5 mg/kg, with equivalent dosages of 3 mg/kg cytarabine) intravenously. During the treatment timeline, the body weights of mice were collected every 2 days. After the C1498-luc cells injection 24 days, mice were sacrificed. The blood samples and major tissues (femur, heart, liver, spleen, lung, and kidney) were collected for further analysis ($n = 3$). The H&E staining was used to detect pathological state.

10^5 C1498-luc cells were intravenously administrated in C57BL/6J mice for survival curves collection. After 7 days injection, mice were randomly divided into six groups ($n = 8$): (1) PBS, (2) SAR317461 (3 mg/kg), (3) CLS (5 mg/kg, with equivalent dosages of 3 mg/kg SAR317461), (4) cytarabine (3 mg/kg), (5) LCS (5 mg/kg, with equivalent dosages of 3 mg/kg cytarabine), and (6) CLCS (5 mg/kg, with equivalent dosages of 3 mg/kg cytarabine) intravenously.

Biosafety Assay. Healthy mice ($n = 3$) were administrated with PBS, SAR317461 (3 mg/kg), CLS (5 mg/kg, with equivalent dosages of SAR317461), cytarabine (3 mg/kg), LCS (5 mg/kg, with equivalent dosages of 3 mg/kg cytarabine), and CLCS (5 mg/kg, with equivalent dosages of 3 mg/kg cytarabine) intravenously. After 48 h treatment, the blood samples of treated-healthy mice were obtained and detected by an Auto Hematology Analyzer (MC-6200VET)

https://doi.org/10.1021/acsomega.4c00710
ACS Omega 2024, 9, 37901−37909

and Blood Biochemistry Analyzer (MNCHIP POINTCARE) for blood routine and blood biochemistry assay.

Statistical Analysis. All data in this study were presented as means ± SD. Statistical significance between two groups was counted by two-tailed unpaired student's *t*-test. Statistical significance among multiple groups was achieved via one-way analysis of variance (ANOVA) using the Tukey posttest or two-way ANOVA using the Tukey posttest. $*p < 0.05$, $**p < 0.01$, and $***p < 0.001$.

■ ASSOCIATED CONTENT

Data Availability Statement

The data underlying this study are available in the published article and its Supporting Information.

Supporting Information

The Supporting Information is available free of charge at https://pubs.acs.org/doi/10.1021/acsomega.4c00710.

Relative quantification of pJAK2, JAK2, pSTAT3, and STAT3 expression; original data of Western blot bands; and H&E staining of major organs in AML-bearing mice (PDF)

■ AUTHOR INFORMATION

Corresponding Author

Xiang Lu − *Department of Hematology, The First People's Hospital of Nanning, Guangxi 530022, P. R. China; The Fifth Affiliated Hospital of Guangxi Medical University, Guangxi 537406, P. R. China*; Email: lyq2829408@126.com

Authors

Yao Zuo − *Department of Hematology & Oncology, Affiliated Hospital of Youjiang Medical University for Nationalities, Guangxi 533000, P. R. China*; orcid.org/0000-0002-7749-2053

Hongwen Li − *Department of Hematology & Oncology, Affiliated Hospital of Youjiang Medical University for Nationalities, Guangxi 533000, P. R. China*

Xiaochao Wang − *Department of Hematology & Oncology, Affiliated Hospital of Youjiang Medical University for Nationalities, Guangxi 533000, P. R. China*

Yejin Liang − *Department of Hematology & Oncology, Affiliated Hospital of Youjiang Medical University for Nationalities, Guangxi 533000, P. R. China*

Caihong Huang − *Department of Hematology & Oncology, Affiliated Hospital of Youjiang Medical University for Nationalities, Guangxi 533000, P. R. China*

Guanye Nai − *Department of Hematology & Oncology, Affiliated Hospital of Youjiang Medical University for Nationalities, Guangxi 533000, P. R. China*

Jingrong Ruan − *Department of Hematology & Oncology, Affiliated Hospital of Youjiang Medical University for Nationalities, Guangxi 533000, P. R. China*

Wenzheng Dong − *Department of Hematology & Oncology, Affiliated Hospital of Youjiang Medical University for Nationalities, Guangxi 533000, P. R. China*

Complete contact information is available at: https://pubs.acs.org/10.1021/acsomega.4c00710

Author Contributions

[§]Y.Z., H.W.L., and X.C.W. contributed equally to this work. Y.Z. performed experiments, analyzed data, as well as wrote the manuscript. Y.Z., H.W.L., X.C.W., and Y.J.L. participated in animal experiments and data analysis. Y.Z., H.W.L., C.H.H., and G.Y.N. participated in the figure preparations. Y.Z., X.C.W., and J.R.R. provided advice on experimental design and provided critical review and editing of manuscript. W.Z.D. and X.L. designed and supervised the research and edited the manuscript. All authors read and approved the final manuscript.

Notes

The authors declare no competing financial interest.

■ ACKNOWLEDGMENTS

This work was supported by grants from the National Science Foundation Project of China (81460026).

■ REFERENCES

(1) Jaeger, A.; Gambheer, S. M. M.; Sun, X. Y.; Chernyakov, D.; Skorobohatko, O.; Mack, T. M.; Kissel, S.; Pfeifer, D.; Zeiser, R.; Fisch, P.; Andrieux, G.; Bräuer-Hartmann, D.; Bauer, M.; Schulze, S.; Follo, M.; Boerries, M.; von Bubnoff, N.; Miething, C.; Hidalgo, J. V.; Klein, C.; Weber, T.; Wickenhauser, C.; Binder, M.; Dierks, C. Activated granulocytes and inflammatory cytokine signaling drive T-cell lymphoma progression and disease symptoms. *Blood* **2023**, 2022015653.

(2) Coombs, C. C.; Tallman, M. S.; Levine, R. L. Molecular therapy for acute myeloid leukaemia. *Nat. Rev. Clin. Oncol.* **2016**, *13*, 305−318.

(3) Guo, Y. L.; Ma, D.; He, Z. C.; Xiong, J.; Kuang, X. Y.; Wang, W. L.; Yu, K. L.; Zhang, Z. Y.; Wang, J. S. Silencing HDAC3 enhances apoptosis of acute B lymphoblastic leukemia cells smurf2 inducing by inhibiting JAK/STAT3 signal pathway. *Blood* **2018**, *132*, 5128.

(4) Zhu, D. R.; Chen, C.; Liu, X. Q.; Wang, S. B.; Zhu, J. M.; Zhang, H.; Kong, L. Y.; Luo, J. G. Osteosarcoma cell proliferation suppression via SHP-2-mediated inactivation of the JAK/STAT3 pathway by tubocapsenolide A. *J. Adv. Res.* **2021**, *34*, 79−91.

(5) Alas, S.; Bonavida, B. Inhibition of constitutive STAT3 activity sensitizes resistant non-Hodgkin's lymphoma and multiple myeloma to chemotherapeutic drug-mediated apoptosis. *Clin. Cancer Res.* **2003**, *9*, 316−326.

(6) Sakamoto, K. M.; Grant, S.; Saleiro, D.; Crispino, J. D.; Hijiya, N.; Giles, F.; Platanias, L.; Eklund, E. A. Targeting novel signaling pathways for resistant acute myeloid leukemia. *Mol. Genet. Metab.* **2015**, *114*, 397−402.

(7) Furqan, M.; Mukhi, N.; Lee, B.; Liu, D. L. Dysregulation of JAK-STAT pathway in hematological malignancies and JAK inhibitors for clinical application. *Biomark. Res.* **2013**, *1*, 5.

(8) Huynh, J.; Etemadi, N.; Hollande, F.; Ernst, M.; Buchert, M. The JAK/STAT3 axis: A comprehensive drug target for solid malignancies. *Semin. Cancer Biol.* **2017**, *45*, 13−22.

(9) Sau, S.; Mondal, S. K.; Kashaw, S. K.; Iyer, A. K.; Banerjee, R. Combination of cationic dexamethasone derivative and STAT3 inhibitor (WP1066) for aggressive melanoma: a strategy for repurposing a phase I clinical trial drug. *Mol. Cell. Biochem.* **2017**, *436*, 119−136.

(10) Ochi, N.; Isozaki, H.; Takeyama, M.; Singer, J. W.; Yamane, H.; Honda, Y.; Kiura, K.; Takigawa, N. Synergistic effect of pacritinib with erlotinib on JAK2-mediated resistance in epidermal gowth factor receptor mutation-positive non-small cell lung cancer. *Exp. Cell Res.* **2016**, *344*, 194−200.

(11) Younes, A.; Romaguera, J.; Fanale, M.; McLaughlin, P.; Hagemeister, F.; Copeland, A.; Neelapu, S.; Kwak, L.; Shah, J.; de Castro Faria, S.; Hart, S.; Wood, J.; Jayaraman, R.; Ethirajulu, K.; Zhu, J. Phase I study of a novel oral Janus kinase 2 inhibitor, SB1518, in patients with relapsed lymphoma: evidence of clinical and biologic activity in multiple lymphoma subtypes. *J. Clin. Oncol.* **2012**, *30*, 4161−4167.

(12) Hayakawa, F.; Sugimoto, K.; Harada, Y.; Hashimoto, N.; Ohi, N.; Kurahashi, S.; Naoe, T. A novel STAT inhibitor, OPB-31121, has a significant antitumor effect on leukemia with STAT-addictive oncokinases. *Blood Cancer J.* **2013**, *3*, No. e166.
(13) Zhang, J. Y.; Wang, Y. T.; Yin, C. J.; Gong, P.; Zhang, Z. W.; Zhao, L. X.; Waxman, S.; Jing, Y. K. Artesunate improves venetoclax plus cytarabine AML cell targeting by regulating the Noxa/Bim/Mcl-1/p-Chk1 axis. *Cell Death Dis.* **2022**, *13*, 379.
(14) Filipczak, N.; Pan, J. Y.; Yalamarty, S. S. K.; Torchilin, V. P. Recent advancements in liposome technology. *Adv. Drug Delivery Rev.* **2020**, *156*, 4−22.
(15) Belfiore, L.; Saunders, D. N.; Ranson, M.; Thurecht, K. J.; Storm, G.; Vine, K. L. Towards clinical translation of ligand-functionalized liposomes in targeted cancer therapy: Challenges and opportunities. *J. Controlled Release* **2018**, *277*, 1−13.
(16) Legrand, O.; Perrot, J. Y.; Baudard, M.; Cordier, A.; Lautier, R.; Simonin, G.; Zittoun, R.; Casadevall, N.; Marie, J. P. The immunophenotype of 177 adults with acute myeloid leukemia: proposal of a prognostic score. *Blood* **2000**, *96*, 870−877.
(17) Linenberger, M. L. CD33-directed therapy with gemtuzumab ozogamicin in acute myeloid leukemia: progress in understanding cytotoxicity and potential mechanisms of drug resistance. *Leukemia* **2005**, *19*, 176−182.
(18) Lee, H. J.; Zhuang, G.; Cao, Y.; Du, P.; Kim, H. J.; Settleman, J. Drug resistance via feedback activation of Stat3 in oncogene-addicted cancer cells. *Cancer Cell* **2014**, *26*, 207−221.

https://doi.org/10.1021/acsomega.4c00710
ACS Omega 2024, 9, 37901−37909